CHAPTER 3

INVESTIGATION ON MGL THERMOELASTICITY THEORY FOR SOME HEAT SOURCE PROBLEMS

3.1 Introduction[1]

The Dirac-delta function is a useful mathematical tool for accurately describing many physical and mechanical processes. The mathematical modeling of the bending and vibration behavior of structures subjected to concentrated loads, impulsive loading, and moving loads, as well as the thermoelastic vibration behavior of structures exposed to heat source, and many more condition may be achieved by the use of the Dirac-delta function. The Dirac-delta function, which was first introduced by theoretical physicist Paul Dirac (1927), is a generalized singularity function that has zero value everywhere except one point, with an integral of one over the entire domain. The most important property of the Dirac delta function is its shifting property. This property allows the delta function to act as a "filter" that extracts the value of a function at a specific point, i.e.

$$\int_{-\infty}^{\infty} f(x)\,\delta(x-\xi)\,dx = f(a)$$

In the context of heat sources, this property allows the extraction of temperature

[1]The content of this subchapter is published in ***Journal of Thermal Stresses***, 46.11 (2023): 1164-1179.

or heat flux at a specific point, simplifying the analysis of localized effects to model the situation involving various heat source scenarios, including point sources, line sources, moving heat source, or periodically varying heat source. This adaptability makes Dirac delta function a valuable tool for representing a wide range of heat input configurations in mathematical models as described below.

Point heat source:

The expression for a time dependent point heat source (Q) at a specific location x_0 can be written as:

$$Q(x,t) = Q_0 \delta(x - x_0) f(t) \tag{3.1.1}$$

$f(t)$ is a function representing the temporal behavior of the heat source. This formulation is suitable for scenarios where the heat source is concentrated at a specific point in space and its intensity can vary with time.

Line heat source:

$$Q(x,t) = Q_0 \delta(x - x_0) h(x) f(t) \tag{3.1.2}$$

the spatial function $h(x)$ represents the intensity of heat source varying along the line.

Moving heat source:

In this case, the idea is to use the Dirac delta function to model the heat source's concentrated nature at a specific position that changes with time due to the motion of the source, i.e.

.

$$Q(x,t) = Q_0 \delta(x - x_0 - vt) g(t) \tag{3.1.3}$$

This expression implies that the heat source is moving with a constant velocity v. $\delta(x - x_0 - vt)$, the Dirac delta function ensures that the heat source is localized at the position $x_0 + vt$ at any time t and the temporal function $g(t)$ represents how the intensity varies with time.

Periodically varying heat source:

Let's consider a heat source that varies periodically of time with a sinusoidal profile.

$$Q = Q_0 \delta\left(t - nL\right) sin\left(\omega t\right) k\left(x\right) \tag{3.1.4}$$

The above expression implies that impulse is applied at specific instances in time when $t = nL$ (where n is an integer), creating a periodic variation. Here, $k\left(x\right)$ is a spatial function that represents how the heat source varies across the material.

In the previous chapter, the strain and temperature rate dependent (MGL) thermoelasticity theory has investigated by considering a problem of thermal shock and some important observations have been pointed out. The present Chapter consisting of two subchapters further deals with the study of MGL theory by considering two different problems of thermoelastic interactions due to the presence of different heat sources and provide the analytical as well as numerical results of the problems. A detailed analysis on the results predicted by this model is presented.

3.2 Investigation on Effects of Strain and Temperature Rates on Thermoelastic Interactions due to Line Heat Source

In this subchapter, the effects of line heat source on a linear, homogeneous and isotropic unbounded elastic medium, which is situated at its centre (origin) is investigated. It is important to mention here that Sherief et al. (1986), Ezzat (1995), Chandrasekharaiah et al. (1991), Chandrasekhariah and Srinath (1998), Dhaliwal et al. (1997), Prasad et al. (2011), Abouelregal et al. (2020) and Singh et al. (2021) have discussed the thermal and elastic behaviour of an unbounded medium in the presence of line heat source with respect to LS, GL, GN-II, GN-III, three phase-lags and QMGT theories, respectively. Experimentally, it has been detected that the wave-like phenomenon oc-

curs for a very short duration of time period (Chandrasekharaiah (1998)). Therefore, we make an effort to derive the asymptotic analytic solution for a very short time in space-time domain. We implement Laplace transform method followed by potential function technique to derive the fundamental solution in the Laplace domain. Finally, we obtain the Laplace inversion analytically through asymptotic expansion by taking Laplace transform domain parameter to be very large. Further, we visualize the analytical results through graphical demonstration with a suitable example. The outcome of current study is discussed in detail with respect to the corresponding results in the contexts of other well-established models (LS and GL models) and this comparative analysis shows how strain rate term plays a consequential role in thermal and elastic wave propagation. Here analytical results, as well as graphical plots for the distribution of displacement field show continuity nature. Moreover, this model indicates an infinite speed of disturbance that decays exponentially.

3.2.1 Problem formulation

This subchapter evaluates the effect of a continuous line heat source located at the origin within an isotropic and homogeneous thermoelastic solid medium that encompasses the whole space. In the given scenario, we consider a medium that exhibits a symmetrical structure corresponding to the z-axis. This medium is subjected to axisymmetric thermoelastic interactions. The field variable displacement, denoted as u, is merely characterized by radial motion. The stress tensor σ_{rr} and $\sigma_{\phi\phi}$ represent the stresses experienced by the body along the radial and transverse directions, respectively. The generalized thermoelasticity theory, as developed by Yu et al. (2018), is formulated within a cylindrical framework defined by the coordinates (r, ϕ, z). The accompanying condition, as mentioned above, can be expressed through Figure (3.2.1).

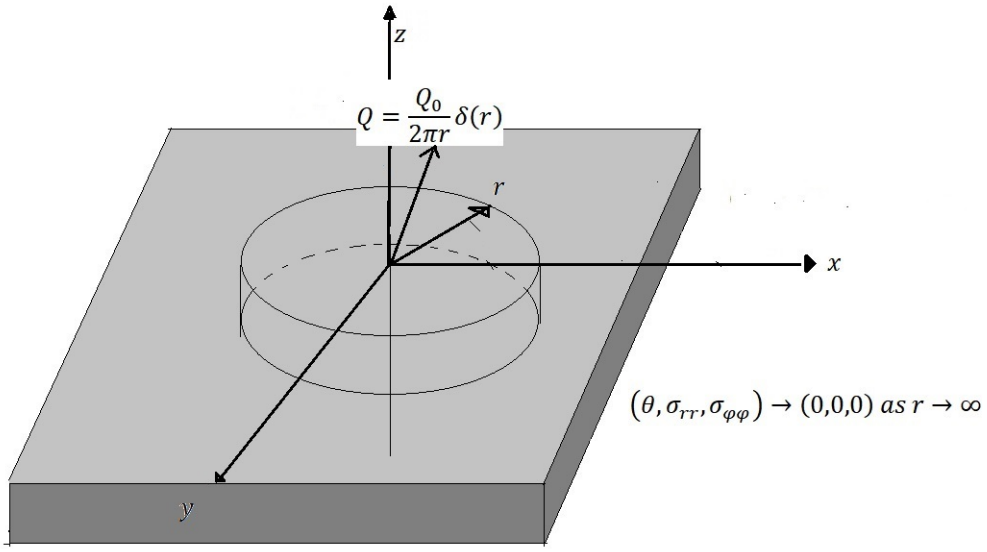

Figure 3.2.1: Infinite solid medium containing line heat source at origin

By following Eqs. (2.3.4-2.3.7) as given in Chapter 2 one can formulate the basic equations in the present context as follows:

Equation of motion in the absence of body force:

$$\rho\frac{\partial^2 u}{\partial t^2} = (1+\tau_1\frac{\partial}{\partial t})\left\{(2\mu+\lambda)\frac{\partial e}{\partial r} - \gamma\frac{\partial \theta}{\partial r}\right\} \tag{3.2.1}$$

The heat conduction equation in presence of heat source (Q):

$$k\left(\frac{\partial^2\theta}{\partial r^2} + \frac{1}{r}\frac{\partial\theta}{\partial r}\right) = \rho c_E(\frac{\partial\theta}{\partial t} + \tau_0\frac{\partial^2\theta}{\partial t^2}) + \gamma T_0(1+\tau_0\frac{\partial}{\partial t})\frac{\partial e}{\partial t} - Q \tag{3.2.2}$$

Stress-displacement-temperature relation:

$$\sigma_{rr} = (1+\tau_1\frac{\partial}{\partial t})\left[(\lambda+2\mu)\frac{\partial u}{\partial r} + \lambda\frac{u}{r} - \gamma\theta\right] \tag{3.2.3}$$

$$\sigma_{\phi\phi} = (1+\tau_1\frac{\partial}{\partial t})\left[(\lambda+2\mu)\frac{u}{r} + \lambda\frac{\partial u}{\partial r} - \gamma\theta\right] \tag{3.2.4}$$

where dilatation is given by

$$e = \frac{\partial u}{\partial r} + \frac{u}{r}. \tag{3.2.5}$$

Let us assume the line heat source of intensity Q_0 located at the origin, which is clearly depicted in Figure (3.2.1).

$$Q = \frac{Q_0}{2\pi r}\delta(r)\, H(t) \tag{3.2.6}$$

In the context of the problem considered, the initial conditions at $t = 0$ are taken in the form (Ezzat (1995)):

$$\begin{aligned} \theta(r,0) = \tfrac{\partial\theta}{\partial t}(r,0) = u(r,0) = \tfrac{\partial u}{\partial t}(r,0) = 0, \\ \sigma_{rr}(r,0) = \tfrac{\partial\sigma_{rr}}{\partial t}(r,0) = \sigma_{\phi\phi}(r,0) = \tfrac{\partial\sigma_{\phi\phi}}{\partial t}(r,0) = 0 \end{aligned} \tag{3.2.7}$$

and the boundary conditions are taken as

$$(\theta, \sigma_{rr}, \sigma_{\phi\phi}) \to (0,0,0) \text{ as } r \to \infty, \tag{3.2.8}$$

where, $H(t)$ is the Heaviside unit step function and $\delta(r)$ is the Dirac delta function. In order to simplify the derivations, we employ the following relationships to convert Eqs. (3.2.1-3.2.4) into dimensionless forms:

$$(r^\star) = v\omega(r), (t^\star) = v^2\omega(t), (\sigma_{rr}^\star) = \frac{(\sigma_{rr})}{(2\mu+\lambda)},$$

$$(\theta^\star) = \frac{(\theta)}{T_0}, (u^\star) = v\omega(u), (Q^\star) = \frac{(Q)}{kT_0(v\omega)^2}$$

where $v = \sqrt{\frac{(2\mu+\lambda)}{\rho}}$ and $\omega = \frac{\rho C_E}{k}$

Therefore, the non-dimensional form of above equations can be achieved as follows.

$$\frac{\partial^2 u}{\partial t^2} = (1 + \tau_1\frac{\partial}{\partial t})\left(\frac{\partial e}{\partial r} - d_1\frac{\partial\theta}{\partial r}\right) \tag{3.2.9}$$

$$\left(\frac{\partial^2\theta}{\partial r^2}+\frac{1}{r}\frac{\partial\theta}{\partial r}\right)=(1+\tau_0\frac{\partial}{\partial t})\frac{\partial}{\partial t}\left(\theta+d_2e\right)-Q \tag{3.2.10}$$

$$\sigma_{rr}=(1+\tau_1\frac{\partial}{\partial t})\left[\frac{\partial u}{\partial r}+\lambda_1\frac{u}{r}-d_1\theta\right] \tag{3.2.11}$$

$$\sigma_{\phi\phi}=(1+\tau_1\frac{\partial}{\partial t})\left[\lambda_1\frac{\partial u}{\partial r}+\frac{u}{r}-d_1\theta\right] \tag{3.2.12}$$

where $d_1=\frac{\gamma T_0}{(2\mu+\lambda)}$, $d_2=\frac{\gamma}{\rho C_E}$, $\lambda_1=\frac{\lambda}{(2\mu+\lambda)}$. In above equations, the superscript $(\star)$ sign has been dropped for the sake of convenience.

Now we shall consider the thermoelastic potential function denoted as φ which is defined by the given relation

$$u=\frac{\partial\varphi}{\partial r} \tag{3.2.13}$$

Using Eq. (3.2.13) in Eqs. (3.2.9-3.2.12), we have

$$\frac{\partial^2\varphi}{\partial t^2}=\left(1+\tau_1\frac{\partial}{\partial t}\right)\left(\nabla^2\varphi-d_1\theta\right) \tag{3.2.14}$$

$$\nabla^2\theta=\left[1+\tau_0\frac{\partial}{\partial t}\right]\left[\frac{\partial\theta}{\partial t}+d_2\frac{\partial}{\partial t}\left(\nabla^2\varphi\right)\right]-Q \tag{3.2.15}$$

$$\sigma_{rr}=\left[1+\tau_1\frac{\partial}{\partial t}\right]\left[\frac{\partial^2\varphi}{\partial r^2}+\lambda_1\frac{1}{r}\frac{\partial\varphi}{\partial r}-d_1\theta\right] \tag{3.2.16}$$

$$\sigma_{\phi\phi}=\left[1+\tau_1\frac{\partial}{\partial t}\right]\left[\lambda_1\frac{\partial^2\varphi}{\partial r^2}+\frac{1}{r}\frac{\partial\varphi}{\partial r}-d_1\theta\right] \tag{3.2.17}$$

where $\nabla^2=\frac{\partial^2}{\partial r^2}+\frac{1}{r}\frac{\partial}{\partial r}$

Replacing θ from Eqs. (3.2.14) and (3.2.15), we have

$$\left[\left(1+\tau_1\frac{\partial}{\partial t}\right)\nabla^4-\left(1+\tau_0\frac{\partial}{\partial t}\right)\left\{(1+d_1d_2)\frac{\partial}{\partial t}\left(1+\tau_1\frac{\partial}{\partial t}\right)\nabla^2+\frac{\partial}{\partial t^3}\right\}\right]\varphi=-d_1\left(1+\tau_1\frac{\partial}{\partial t}\right)Q. \tag{3.2.18}$$

Eq. (3.2.14) can be re-written as

$$d_1\left(1+\tau_1\frac{\partial}{\partial t}\right)\theta=\left(1+\tau_1\frac{\partial}{\partial t}\right)\left(\nabla^2\varphi\right)-\frac{\partial^2\varphi}{\partial t^2}. \tag{3.2.19}$$

Eliminating θ from Eqs. (3.2.16) and (3.2.17) and by using Eq. (3.2.19), we have

$$\sigma_{rr} = \left[1 + \tau_1 \frac{\partial}{\partial t}\right] \left[\frac{(\lambda_1 - 1)}{r} \frac{\partial \varphi}{\partial r}\right] + \frac{\partial^2 \varphi}{\partial t^2}. \tag{3.2.20}$$

$$\sigma_{\phi\phi} = \left[1 + \tau_1 \frac{\partial}{\partial t}\right] \left[(\lambda_1 - 1) \frac{\partial^2 \varphi}{\partial r^2}\right] + \frac{\partial^2 \varphi}{\partial t^2}. \tag{3.2.21}$$

3.2.2 Solution in the Laplace transform domain

In this particular subsection, our problem is effectively addressed by employing the Laplace transform technique corresponding to the time variable. The initial condition Eq. (3.2.7) can be represented as

$$\varphi = \frac{\partial \varphi}{\partial t} = \frac{\partial^2 \varphi}{\partial t^2} = \frac{\partial^3 \varphi}{\partial t^3} = 0, \text{ at } t = 0 \tag{3.2.22}$$

while the boundary condition (3.2.8) can be written as

$$\left(\varphi, \frac{\partial \varphi}{\partial r}, \frac{\partial^2 \varphi}{\partial r^2}\right) \to (0, 0, 0) \text{ as } r \to \infty. \tag{3.2.23}$$

Taking Laplace transform to Eqs. (3.2.13) and (3.2.18-3.2.21), we have

$$\overline{u} = \frac{\partial \overline{\varphi}}{\partial r} \tag{3.2.24}$$

$$\left[\nabla^4 - \left\{\frac{b_1 s^3 + b_2 s^2 + b_3 s}{1 + \tau_1 s}\right\} \nabla^2 + \frac{s^3 (1 + \tau_0 s)}{1 + \tau_1 s}\right] \overline{\varphi} = -\frac{A_1 d_1 \delta(r)}{rs} \tag{3.2.25}$$

$$d_1 (1 + \tau_1 s) \overline{\theta} = (1 + \tau_1 s) \left(\nabla^2 \overline{\varphi}\right) - s^2 \overline{\varphi} \tag{3.2.26}$$

$$\overline{\sigma}_{rr} = [1 + \tau_1 s] \left[\frac{(\lambda_1 - 1)}{r} \frac{\partial \overline{\varphi}}{\partial r}\right] + s^2 \overline{\varphi} \tag{3.2.27}$$

$$\overline{\sigma}_{\phi\phi} = [1 + \tau_1 s] \left[(\lambda_1 - 1) \frac{\partial^2 \overline{\varphi}}{\partial r^2}\right] + s^2 \overline{\varphi} \tag{3.2.28}$$

where $A_1 = \frac{Q_0}{2\pi}, b_1 = (1 + d_1 d_2)\,\tau_1\tau_0, b_2 = (1 + d_1 d_2)\,(\tau_1 + \tau_0) + 1, b_3 = 1 + d_1 d_2$.

Eq. (3.2.25) can be re-written as

$$\left(\nabla^2 - w_1^2\right)\left(\nabla^2 - w_2^2\right)\overline{\varphi} = -\frac{A_1 d_1 \delta\,(r)}{rs}. \tag{3.2.29}$$

Here w_1^2 and w_2^2 are the roots of the equation:

$$x^2 - \left\{\frac{b_1 s^3 + b_2 s^2 + b_3 s}{1 + \tau_1 s}\right\} x + \frac{s^3\,(1 + \tau_0 s)}{1 + \tau_1 s} = 0 \tag{3.2.30}$$

With the help of the boundary conditions (3.2.23), the solution of Eq. (3.2.29) can be written by

$$\overline{\varphi} = \frac{A_1 a_1}{s\,(w_1^2 - w_2^2)} \sum_{i=1}^{2} (-1)^{i+1} K_0\,(w_i r) \tag{3.2.31}$$

where $K_0\,(w_i r)$ is the modified Bessel function of the second kind of order zero.

By putting Eq. (3.2.31) into Eqs. (3.2.24) and (3.2.26-3.2.28), and using the subsequent mathematical relationships,

$$\frac{\partial}{\partial r} k_0\,(ar) = -a k_1\,(ar)\,, \nabla^2 k_0\,(ar) = a^2 k_0\,(ar)\,, \frac{\partial^2}{\partial r^2} k_0\,(ar) = a^2 k_0\,(ar) + \frac{a}{r} k_1\,(ar)\,,$$

we get

$$\overline{u}\,(r, s) = \frac{-A_1 d_1}{s\left(w_1^2 - w_2^2\right)} \sum_{i=1}^{2} (-1)^{i+1}\, n_i K_1\,(w_i r) \tag{3.2.32}$$

$$\overline{\theta}\,(r, s) = \frac{A_1}{s\left(w_1^2 - w_2^2\right)} \sum_{i=1}^{2} (-1)^{i-1} \left(n_i^2 - \frac{s^2}{1 + \tau_1 s}\right) K_0\,(w_i r) \tag{3.2.33}$$

$$\overline{\sigma}_{rr}\,(r, s) = \frac{(1 + \tau_1 s)\,A_1 d_1}{s\left(w_1^2 - w_2^2\right)} \sum_{i=1}^{2} (-1)^{i+1} \left\{\frac{s^2}{1 + \tau_1 s} K_0\,(w_i r) + \left(\frac{n_i}{r}\right)(1 - \lambda_1)\, K_1\,(w_i r)\right\} \tag{3.2.34}$$

$$\overline{\sigma}_{\phi\phi}(r,s) = \frac{(1+\tau_1 s) A_1 d_1}{s\left(w_1^2 - w_2^2\right)} \sum_{i=1}^{2} (-1)^{i-1} \left[\left\{ (\lambda_1 - 1) n_i^2 + \frac{s^2}{(1+\tau_1 s)} \right\} K_0(w_i r) - n_i \left(\frac{1-\lambda_1}{r} \right) K_1(w_i r) \right] \tag{3.2.35}$$

The Eqs. (3.2.32-3.2.35) provide the required solutions of the current problem in the Laplace transform domain (r, s). In the following sections, we will determine the analytical solution to this problem in the space-time domain. Additionally, we will examine the impact of the heat source and compare the predictions of the current model with other established models found in the existing literature.

3.2.3 Small-time approximated solution in (r, t) domain

In the preceding subsection, the derived fundamental solution encompasses the expressions that incorporate the Laplace transform parameter s. Therefore, the acquisition of closed form analytical solutions in the physical domain appears to be an exceedingly challenging task. The theory under consideration finds practical applications primarily in short-time experiments, primarily due to the inclusion of relaxation parameters, which are characterized by exceedingly small values. Considering the aforementioned fact, our focus will be directed towards determining the short-time approximations of the field variables by means of Taylor series expansion. The expression for the roots of Eq. (3.2.30) can be derived as follows.

$$w_i = \left\{ \frac{\left(b_1 s^3 + b_2 s^2 + b_3 s\right) \pm \sqrt{\left(b_1 s^3 + b_2 s^2 + b_3 s\right)^2 - 4 s^3 (1+\tau_0 s)(1+\tau_1 s)}}{2(1+\tau_1 s)} \right\}^{1/2} \tag{3.2.36}$$

After conducting rigorous manipulations, we have determined that m_1 and m_2 represent the approximations for w_1 and w_2 respectively. These approximations are expressed in the subsequent forms:

$$m_1 = a_{61}s + a_{62} + \frac{a_{63}}{s} \tag{3.2.37}$$

$$m_2 = a_{81}\sqrt{s} + \frac{a_{82}}{\sqrt{s}} + \frac{a_{83}}{s^{3/2}} \tag{3.2.38}$$

where

$$a_{61} = \sqrt{a_{51}},\ a_{62} = \frac{a_{52}}{2\sqrt{a_{51}}},\ a_{63} = \frac{-a_{52}a_{52} + 4a_{51}a_{53}}{8\left(a_{51}\right)^{3/2}},$$

$$a_{81} = \sqrt{a_{71}},\ a_{82} = \frac{a_{72}}{2\sqrt{a_{71}}},\ a_{83} = \frac{-a_{72}a_{72} + 4a_{71}a_{73}}{8\left(a_{71}\right)^{3/2}},$$

$$a_{71} = \frac{a_{41}}{2\tau_1}, a_{72} = \frac{-a_{41} + a_{42}\tau_1}{2\left(\tau_1\right)^2}, a_{73} = \frac{a_{41} - a_{42}\tau_1 + a_{43}\left(\tau_1\right)^2}{2\left(\tau_1\right)^3},$$

$$a_{51} = \frac{a_{31}}{2\tau_1}, a_{52} = \frac{-a_{31} + a_{32}\tau_1}{2\left(\tau_1\right)^2}, a_{53} = \frac{a_{31} - a_{32}\tau_1 + a_{33}\left(\tau_1\right)^2}{2\left(\tau_1\right)^3},$$

$$a_{31} = 2b_1, a_{32} = b_2 + \frac{a_{12}}{2\sqrt{a_{11}}}, a_{33} = b_3 + \frac{-a_{12}^2 + 4a_{11}a_{13}}{8a_{11}^{\frac{3}{2}}},$$

$$a_{41} = b_2 - \frac{a_{12}}{2\sqrt{a_{11}}}, a_{42} = b_3 - \frac{\left(-a_{12}^2 + 4a_{11}a_{13}\right)}{8a_{11}^{\frac{3}{2}}}, a_{43} = -\frac{\left(a_{12}^3 - 4a_{11}a_{12}a_{13} + 8a_{11}^2a_{14}\right)}{16a_{11}^{\frac{5}{2}}},$$

$$a_{11} = b_1^2, a_{12} = 2b_1b_2 - 4\tau_0\tau_1, a_{13} = b_2^2 + 2b_1b_3 - 4(\tau_0 + \tau_1), a_{14} = 2b_2b_3 - 4$$

$$b_1 = \left(1 + d_1d_2\right)\tau_0\tau_1, b_2 = 1 + \left(1 + d_1d_2\right)\left(\tau_0 + \tau_1\right), b_3 = 1 + d_1d_2,$$

Now, we will replace the value of m_i obtained from Eqs. (3.2.37) and (3.2.38) into Eqs. (3.2.32-3.2.35) and simplify the resulting expressions. The expressions of different notations (g_{ij},c_{ij}, h_{ij},) used in below solutions are provided in Appendix II. This will enable us to find the approximate solutions of the field variables in the Laplace Domain,

as

$$\overline{u}\left(r,s\right)=-A_1d_1\sqrt{\frac{\pi}{2r}}\left[e^{-\left(a_{61}s+\frac{a_{63}}{s}\right)r}\{\frac{g_{31}}{s^{\frac{5}{2}}}+\frac{g_{32}}{s^{\frac{7}{2}}}\}+e^{-\left(a_{81}r\sqrt{s}\right)}\{\frac{g_{34}}{s^{\frac{11}{4}}}+\frac{g_{35}}{s^{\frac{13}{4}}}\}\right] \tag{3.2.39}$$

$$\overline{\theta}\left(r,s\right)=A_1d_1\sqrt{\frac{\pi}{2r}}\left[e^{-\left(a_{61}s+\frac{a_{63}}{s}\right)r}\{\frac{c_{71}}{s^{\frac{3}{2}}}+\frac{c_{72}}{s^{\frac{5}{2}}}\}+e^{-\left(a_{81}r\sqrt{s}\right)}\{\frac{c_{81}}{s^{\frac{9}{4}}}+\frac{c_{82}}{s^{\frac{11}{4}}}\}\right] \tag{3.2.40}$$

$$\overline{\sigma}_{rr}\left(r,s\right)=A_1d_1\sqrt{\frac{\pi}{2r}}\left[e^{-\left(a_{61}s+\frac{a_{63}}{s}\right)r}\{\frac{h_{21}}{s^{\frac{3}{2}}}+\frac{h_{22}}{s^{\frac{5}{2}}}\}+e^{-\left(a_{81}r\sqrt{s}\right)}\{\frac{h_{24}}{s^{\frac{5}{4}}}+\frac{h_{25}}{s^{\frac{7}{4}}}\}\right] \tag{3.2.41}$$

$$\overline{\sigma}_{\phi\phi}\left(r,s\right)=A_1a_1\sqrt{\frac{\pi}{2r}}\left[e^{-\left(a_{61}s+\frac{a_{63}}{s}\right)r}\{\frac{h_{91}}{s^{\frac{1}{2}}}+\frac{h_{92}}{s^{\frac{3}{2}}}\}+e^{-\left(a_{81}r\sqrt{s}\right)}\{\frac{h_{94}}{s^{\frac{5}{4}}}+\frac{h_{95}}{s^{\frac{7}{4}}}\}\right] \tag{3.2.42}$$

The solutions in the physical domain (r,t) can be obtained by employing the established standard results for Laplace inversion given by

$$L^{-1}\left\{s^{-n-1}e^{\frac{-b}{s}}\right\}=\left(x/b\right)^{n/2}J_n\left(2\sqrt{bx}\right),\ \ Re\left(n\right)>-1$$

$$L^{-1}\left(s^{-\frac{n}{2}-\frac{1}{2}}e^{-b\sqrt{s}}\right)=\frac{1}{2\sqrt{\pi}\left(b\right)^{n/2}\left(x\right)^{\frac{3}{2}}}\int_0^\infty u^{1+\frac{n}{2}}e^{-\frac{u^2}{4t}}I_n\left(2\sqrt{bu}\right)du,\ Re\left(n\right)>-1,\ Re\left(a\right)>0$$

where J_n and I_n are the Bessel function and modified Bessel function of order n respectively.

Using the preceding formulae, inverse Laplace transform of Eqs. (3.2.39-3.2.42) yields

$$
\begin{aligned}
u(r,t) = -K \Bigg[& H(t-L_{11}) \Bigg\{ g_{31} \left(\frac{sin\left(2\sqrt{L_{12}(t-L_{11})}\right)}{2\sqrt{\pi}(L_{12})^{3/2}} - (t-L_{11})^{1/2} \frac{cos\left(2\sqrt{L_{12}(t-L_{11})}\right)}{\sqrt{\pi}L_{12}} \right) \\
& + g_{32} \Bigg(\left(\frac{1}{L_{12}}\right)^{3/2} (t-L_{11}) \Bigg(-\frac{3cos\left(2\sqrt{L_{12}(t-L_{11})}\right)}{2\sqrt{t-L_{11}}\sqrt{L_{12}}} - -sin\left(2\sqrt{L_{12}(t-L_{11})}\right) \\
& + \frac{3sin\left(2\sqrt{L_{12}(t-L_{11})}\right)}{4(t-L_{11})(L_{12})} \Bigg) \Bigg) \Bigg\} \\
& + \frac{e^{-\frac{L_{21}^2}{8t}}}{\sqrt{t}} \Bigg\{ g_{34} \frac{4\sqrt{L_{21}}}{105} \Bigg[\left(10t^2 + 10tL_{21}^2 + L_{21}^4\right) I_{\frac{-1}{4}}\left(\frac{L_{21}^2}{8t}\right) - \left(L_{21}^4 + 14tL_{21}^2 + 42t^2\right) I_{\frac{1}{4}}\left(\frac{L_{21}^2}{8t}\right) \\
& + \left(L_{21}^4 + 8tL_{21}^2\right) \left(I_{\frac{3}{4}}\left(\frac{L_{21}^2}{8t}\right) - I_{\frac{5}{4}}\left(\frac{L_{21}^2}{8t}\right) \right) \Bigg] \\
& + g_{35} \frac{8}{945\sqrt{L_{21}}} \Bigg[\left(10t^2 + 10tL_{21}^2 + L_{21}^4\right) I_{\frac{-1}{4}}\left(\frac{L_{21}^2}{8t}\right) - \left(42t^2 + 14tL_{21}^2 + L_{21}^4\right) I_{\frac{1}{4}}\left(\frac{L_{21}^2}{8t}\right) \\
& + \left(21t^2L_{21}^2 + 15tL_{21}^4 + L_{21}^6\right) \left(-I_{\frac{3}{4}}\left(\frac{L_{21}^2}{8t}\right) + I_{\frac{5}{4}}\left(\frac{L_{21}^2}{8t}\right) \right) \Bigg] \Bigg\} \Bigg] \qquad (3.2.43)
\end{aligned}
$$

$$
\begin{aligned}
\theta(r,t) = K \Bigg[& H(t-L_{11}) \Bigg\{ c_{71} \frac{sin\left(2\sqrt{L_{12}(t-L_{11})}\right)}{\sqrt{\pi L_{12}}} \\
& + c_{72} \left(\frac{\frac{sin\left(2\sqrt{L_{12}(t-L_{11})}\right)}{2\sqrt{L_{12}}} - (t-L_{11})^{1/2} cos\left(2\sqrt{L_{12}(t-L_{11})}\right)}{\sqrt{\pi}L_{12}} \right) \Bigg\} \\
& + \frac{e^{-\frac{L_{21}^2}{8t}}}{\sqrt{t}} \Bigg\{ c_{81} \frac{2}{15\sqrt{L_{21}}} \Bigg[-\left(5tL_{21}^2 + L_{21}^4\right) I_{\frac{-1}{4}}\left(\frac{L_{21}^2}{8t}\right) + \left(L_{21}^4 + 9tL_{21}^2 + 12t^2\right) I_{\frac{1}{4}}\left(\frac{L_{21}^2}{8t}\right) \\
& + \left(L_{21}^4 + 3tL_{21}^2\right) \left(-I_{\frac{3}{4}}\left(\frac{L_{21}^2}{8t}\right) + I_{\frac{5}{4}}\left(\frac{L_{21}^2}{8t}\right) \right) \Bigg] \\
& + c_{82} \frac{4\sqrt{L_{21}}}{105} \Bigg\{ \left(10t^2 + 10tL_{21}^2 + L_{21}^4\right) I_{\frac{-1}{4}}\left(\frac{L_{21}^2}{8t}\right) - \left(42t^2 + 14tL_{21}^2 + L_{21}^4\right) I_{\frac{1}{4}}\left(\frac{L_{21}^2}{8t}\right) \\
& + \left(L_{21}^4 + 8tL_{21}^2\right) \left(I_{\frac{3}{4}}\left(\frac{L_{21}^2}{8t}\right) - I_{\frac{5}{4}}\left(\frac{L_{21}^2}{8t}\right) \right) \Bigg\} \Bigg\} \Bigg] \qquad (3.2.44)
\end{aligned}
$$

$$\sigma_{rr}(r,t) = K\left[H(t-L_{11})\left\{h_{21}\frac{sin\left(2\sqrt{L_{12}(t-L_{11})}\right)}{\sqrt{\pi L_{12}}}\right.\right.$$
$$\left.+h_{22}\left(\frac{\frac{sin\left(2\sqrt{L_{12}(t-L_{11})}\right)}{2\sqrt{L_{12}}}-(t-L_{11})^{1/2}cos\left(2\sqrt{L_{12}(t-L_{11})}\right)}{\sqrt{\pi}L_{12}}\right)\right\}$$
$$+\frac{e^{-\frac{L_{21}^2}{8t}}}{\sqrt{t}}\left\{\frac{h_{24}}{2\sqrt{L_{21}}}\left\{-L_{21}^2 I_{\frac{-1}{4}}\left(\frac{L_{21}^2}{8t}\right)+\left(L_{21}^2+4t\right)I_{\frac{1}{4}}\left(\frac{L_{21}^2}{8t}\right)\right.\right.$$
$$\left.+L_{21}^2\left(-I_{\frac{3}{4}}\left(\frac{L_{21}^2}{8t}\right)+I_{\frac{5}{4}}\left(\frac{L_{21}^2}{8t}\right)\right)\right\}$$
$$+\frac{h_{25}\sqrt{L_{21}}}{3}\left(\left(L_{21}^2+2t\right)I_{\frac{-1}{4}}\left(\frac{L_{21}^2}{8t}\right)-\left(L_{21}^2+6t\right)I_{\frac{1}{4}}\left(\frac{L_{21}^2}{8t}\right)\right.$$
$$\left.\left.\left.-\left(L_{21}^2+6t\right)I_{\frac{1}{4}}\left(\frac{L_{21}^2}{8t}\right)+L_{21}^2\left(I_{\frac{3}{4}}\left(\frac{L_{21}^2}{8t}\right)-I_{\frac{5}{4}}\left(\frac{L_{21}^2}{8t}\right)\right)\right)\right\}\right] \tag{3.2.45}$$

$$\sigma_{\phi\phi}(r,t) = K\left[H(t-L_{11})\left\{h_{91}\frac{cos\left(2\sqrt{L_{12}(t-L_{11})}\right)}{\sqrt{\pi(t-L_{11})}}+h_{92}\left(\frac{sin\left(2\sqrt{L_{12}(t-L_{11})}\right)}{\sqrt{\pi L_{12}}}\right)\right\}\right.$$
$$+\frac{e^{-\frac{L_{21}^2}{8t}}}{\sqrt{t}}\left\{\frac{h_{94}}{2\sqrt{L_{21}}}\left(-L_{21}^2 I_{\frac{-1}{4}}\left(\frac{L_{21}^2}{8t}\right)+\left(L_{21}^2+4t\right)I_{\frac{1}{4}}\left(\frac{L_{21}^2}{8t}\right)\right.\right.$$
$$\left.+L_{21}^2\left(-I_{\frac{3}{4}}\left(\frac{L_{21}^2}{8t}\right)+I_{\frac{5}{4}}\left(\frac{L_{21}^2}{8t}\right)\right)\right)$$
$$+\frac{h_{95}\sqrt{L_{21}}}{3}\left\{\left(L_{21}^2+2t\right)I_{\frac{-1}{4}}\left(\frac{L_{21}^2}{8t}\right)-\left(L_{21}^2+6t\right)I_{\frac{1}{4}}\left(\frac{L_{21}^2}{8t}\right)\right.$$
$$\left.\left.\left.+L_{21}^2\left(I_{\frac{3}{4}}\left(\frac{L_{21}^2}{8t}\right)-I_{\frac{5}{4}}\left(\frac{L_{21}^2}{8t}\right)\right)\right\}\right\}\right] \tag{3.2.46}$$

where $a_{61}r = L_{11}, a_{63}r = L_{12}, a_{81}r = L_{21}, K = A_1 d_1\sqrt{\frac{\pi}{2r}}$.

The analytical solutions for the distribution of displacement, temperature, and stress components in the physical domain (r,t) over short time in the context of the MGL model are provided by the system of Eqs. (3.2.43-3.2.46). It is important to note that the solution for each field obtained for the present problem incorporates a resultant of a coupled mathematical expressions. These formulas exhibit exponential decline as the radial distance increases. The first expressions attached to the term $H(t-L_{11})$ gives indication of existence of a wave propagating at a non-dimensional finite velocity of $1/a_{61}$. The coefficients a_{61} and a_{62} exhibit the clear dependency of speed and attenuation decay on the material parameters including the relaxation parameters, so implying

that the wave speed and decay coefficient are further influenced by these specified factors. At a given moment of time t, the first component of the expression has an effect upto location $\frac{t}{a_{61}}$ due to presence of Heaviside function. The remaining portion of the expression for the field variables, as expressed in equations (40-43), do not exhibit any discernible participation to the wave effect. Contrary to initial expectations, it exhibits diffusive characteristic and its propagation indicates an exponentially decay pattern with radial distance. Notably, even at considerable distances from the heat source, there is indication of a minimal yet discernible impact. Based on this observation, it can be inferred that the influence of the heat source are not confined up to bounded region. Field variables depend on heat source's strength Q_0. Additionally, it can be clearly observed that in the context of this model, there is a single wavefront where the temperature, displacement, and radial stress components exhibit continuous behavior. However, it is worth noting that the circumferential stress component encounters an infinite jump discontinuity at this particular wavefront.

Furthermore, we compare our results with the corresponding results under other existing thermoelastic models like LS and GL models. By deriving the small time approximation solution for the cases of LS model (Sherief and Anwar (1986)) and GL model (Ezzat (1995)) researchers had reported that the solution for the field variables consists of combination of two waves, and both the waves travel with finite velocity and exponential decay with radial distance. Thus this result shows that on the contrary of the predictions of the MGL model, the effect of line heat source under all these existing theories are confined to a time-dependent finite region of space surrounding the source and two wavefronts exist under these models. In the case of LS model, the temperature and stress component are declared to be discontinuous in nature showing infinite jump discontinuity at both the wavefronts. However, in the case of GL model, the temperature and stress components show finite jump discontinuity at both the wavefronts. Therefore, a significant disagreement is observed in the prediction by the

present MGL thermoelasticity theory as compared to the other existing theories as mentioned above.

3.2.4 Numerical results and discussions

This subsection attempts to explain the aforementioned analytical outcome with the help of graphical representations, and also conduct a comparative analysis of our findings with other thermoelastic models. In Figures (3.2.2-3.2.5), we present the graphical representation of dimensionless field values such as temperature, displacement, and radial and circumferential stresses.

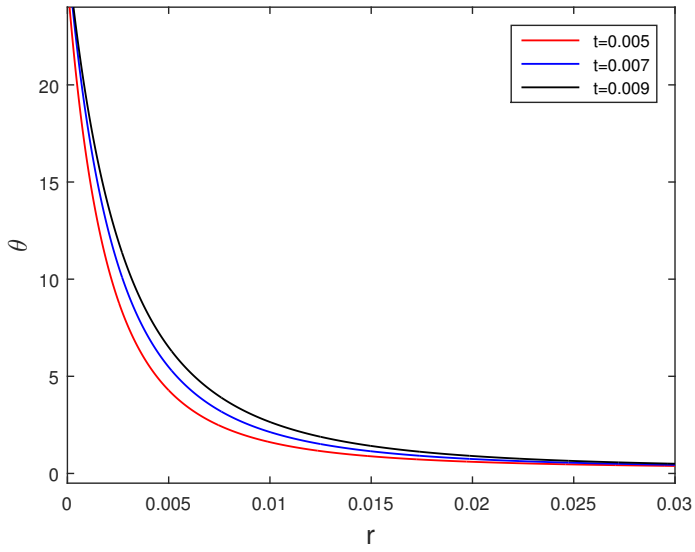

Figure 3.2.2: Variation of dimensionless temperature with radial distance

These figures depict the variation of these quantities with respect to radial distance at three different instants of time. For the convenience of comparison and discussions, the values of relevant parameters used for the numerical computation is of copper material, The physical data for which is given in chapter 2. Non-dimensional relaxation time parameters are taken as $\tau_0 = 0.02$, $\tau_1 = 0.05$.

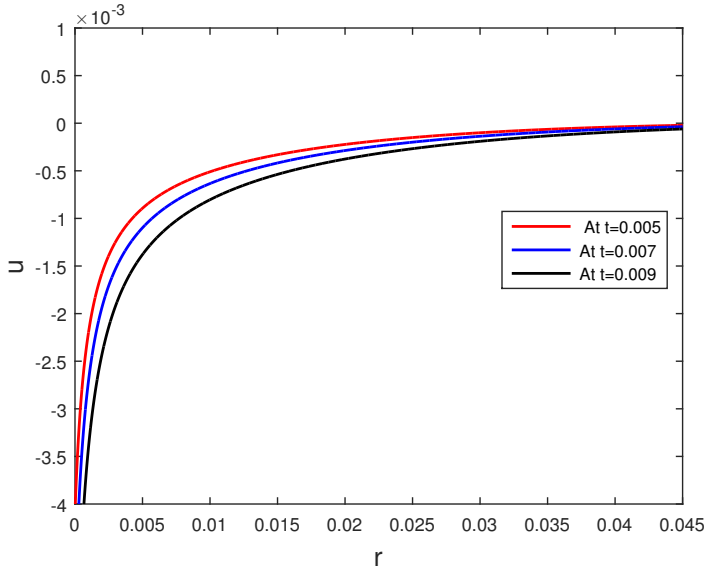

Figure 3.2.3: Variation of dimesionless displacement with radial distance

Figure (3.2.2) demonstrates the temperature variation with respect to r at different instants of time. One can easily note that the temperature field shows very high value near the location of the line heat source and it falls down with radial distance. We find that as time passes, the temperature at particular position increases. The temperature field is observed to be continuous in nature except at the point of origin, which indicate an infinite singularity of the profile. This result matches our analytical result. However, Sherief et al. (1986) and Ezzat (1995) reported certain different behavior of the temperature field under the LS, and GL thermoelastic models, respectively. In these models, existence of two wavefronts have been observed. According to GL model, the temperature field has a finite jump discontinuity at both the wavefronts. In the case of LS model, Sherief et al. (1986) reported that the temperature field has infinite jump discontinuity at both the wavefronts. In both the models (LS and GL), the effect of heat source is observed up to thermal wavefront position and the temperature at particular position starts with a sudden jump. However, like all these models (LS, and GL), the present MGL model indicates the same infinite singularity of the field variables at the

location of the heat source (origin).

The radial variation of displacement is depicted in Figure (3.2.3). The magnitude of displacement exhibits a large (infinite) value at the origin ($r = 0$) and subsequently reduces consistently as the radial distance increases. Thus, similar behavior of displacement field has been investigated by Sherief et al. (1986), Ezzat (1995) for LS and GL models simultaneously. Sherief et al. (1986) and Ezzat (1995) have also examined this phenomenon in the context of both LS and GL models simultaneously. Figures (3.2.4 and 3.2.5) illustrate variations in the radial and circumferential stress components, respectively. It is worth noting that the material experiences a significant compressive stress in close vicinity to the heat source, and this stress falls rapidly as the radial distance increases. The magnitude of stress components is also dependent upon the intensity of the heat source. Figure 5 demonstrates that the circumferential stress component exhibits high compressive stress, characterized by an infinite jump discontinuity, at certain positions along the single wavefront. These regions are identified as $r = 0.034, 0.048$, and 0.062 occurring at time instances $t = 0.005, 0.007$, and 0.009 respectively. Subsequent to this juncture, a significant decline in compressive stress is apparent, ultimately reaching a state of minimal magnitude, approaching zero. The position of discontinuity changes its position with time and has a velocity of $1/a_{61}$. Sherief et al. (1986) and Ezzat (1995) have documented contrasting observations on the stress field components in the context of the LS and GL thermoelastic models, respectively. In the context of GL theory, it is seen that both the radial and circumferential stress components exhibit discontinuities characterized by finite jump behavior at the wavefronts. Moreover, the impact of the heat source has been detected just upto wavefront location of the faster wave, and it varies with time.

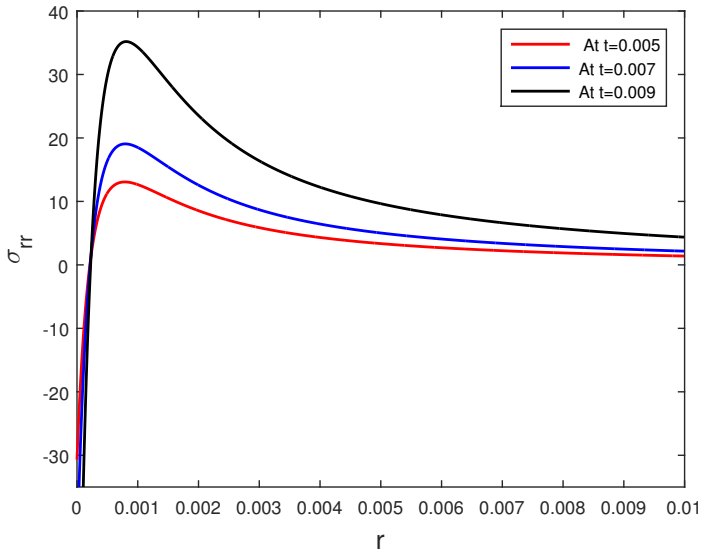

Figure 3.2.4: Variation of dimensionless radial stress with radial distance

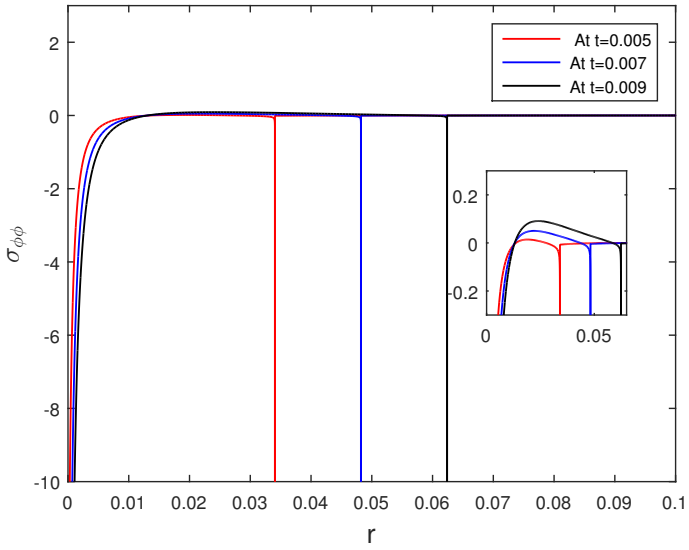

Figure 3.2.5: Variation of dimensionless circumferential stress with radial distance

3.2.5 Conclusions

The main observations in present subchapter is summarized as follows:

- The short-time approximated solution for MGL model reveals that each field variable consists of combination of wave term and diffusive term and it decays exponentially. Due to the diffusive term, the disturbance propagates with infinite speed analogous to classical thermoelasticity theory. For MGL model, the effect of line heat source is observed up to larger domain in comparison to LS,and GL models.

- Unlike the case of present MGL model, the LS, and GL models predict that the impact of the line heat source is confined to a time-dependent finite region of the space surrounding the heat source and admit finite speed of both thermal and elastic waves. Consequently, both waves are damped in nature.

- Unlike the case of GL and LS models, the MGL model predicts that the stress components and temperature are continuous at all points of the medium, except at the origin (location of heat source), leaving circumferential stress component only which is discontinuous at the location of wave front. In LS theory, the temperature and stress distributions show infinite jump discontinuity behavior at the thermal and elastic wavefronts, whereas for GL model, the stress and temperature fields show discontinuity with finite jump at both wavefronts.

- In the case of MGL theory, like LS theory, the continuum hypothesis is satisfied since the distribution of displacement field variable is observed to be continuous in nature throughout the medium.

3.3 Relaxation Effects on Thermoelastic Interactions for Time Dependent Moving Heat Source under MGL Thermoelasticity

3.3.1 Introduction[2]

For most common engineering materials, such as metals, the value of τ is known to be of the order of a picosecond or less. As such, it was believed till nineties that the thermal relaxation effects are of relevance only in specialized applications involving very small time intervals and/or very large heat fluxes. High-rate heating is a rapidly emerging area in heat transfer. Such situations are not impossible even from a practical point of view. For example, in the problem of nucleate boiling, which is of great interest to heat transport engineers, even times of order 10^{-6} s are relevant (Hsu (1962)). Also, time periods as short as 10^{-13} s are of significance in determining temperature rise in crystals caused by exothermic catalytic reactions. Further, laser penetration and welding, explosive bonding and melting are potential areas which give rise to very high heat fluxes. These problems are associated with shortening of the response time, the nonequilibrium thermodynamic transition and the microscopic effects in the energy exchange are two important issues to be faced. An equilibrium state in thermodynamic transitions, first of all, needs time to be established. The response time be comparable or even shorter than that required to establish an equilibrium state, physical mechanisms reflecting the nonequilibrium thermodynamic transition must be addressed in the high-rate model. The relaxation time proposed by Chester (1963) provides a typical example that in an idealized solid, the thermal energy can be transported by quantized electronic excitation, which are called free electrons, and by the quanta of lattice vibra-

[2]The content of this subchapter is published in *Zeitschrift für angewandte Mathematik und Physik*, 72 (2021): 1-13.

tions, which are called phonons. The relaxation time τ is associated with the average communication time between these collisions for the commencement of resistive flow. The relaxation concept based on the critical frequency of molecular collisions places the thermal wave behavior originally hypothesized by Morse and Feshbach (1953), Cattaneo (1958), and Vernotte (1958; 1961) on a firm physical foundation. The phase-lag concept proposed by Tzou (1992; 1993) in essence, is the same effort addressing the nonequilibrium thermodynamic transition from a macroscopic point of view. But now the situation is different. Experimental studies made by Kaminski (1990) on materials with non-homogeneous inner structures have revealed that the value of τ (at laboratory temperatures) is about 11 s for glass ballotini, 21 s for sand, 25 s for H acid, 29 s for NaHCO3, and 54 s for ion exchanger. Studies made by Vedavarz et al. ((1994)) and Mitra et al. (1994) have indicated that τ is equal to about 16 s for processed meat. These studies indicate that the thermal relaxation effects can be of relevance even in, common engineering applications where the time scales of interest are of the order of a fraction of a minute.

The present subchapter is aimed to understand the effects of relaxation parameters due to the incorporation of strain rate as well as the temperature rate terms in modeling the thermoelastic interactions inside a homogeneous, isotropic, unbounded elastic medium with a cylindrical cavity subjected to time-dependent moving heat source and thermal shock. It is worth to be mentioned that the moving heat source problem is widely used in many applications such as laser cutting, boiling, material processing, etc. We refer the investigation by Youssef (2009) for this kind of problem related with generalized thermoelasticity theory. Being motivated to the application of moving heat source problem, we aim to investigate the influence of strain rate as well as the temperature rate in thermoelastic interactions due to thermal shock under MGL model in presence of a moving heat source inside the medium. To study this problem, we combine the governing equations of the strain-temperature rate dependent thermoelasticity

(MGL) theory with other two generalized thermoelasticity theories (GL and LS) and we formulate the problem to derive unified governing equations for these three theories. We assume that the body has an axisymmetric structure and is under the axisymmetric load. The Laplace transform technique is executed to solve the unified system of governing equations. We further employ the Stehfest algorithm (Stehfest (1970)) to find the numerical inversion of Laplace transform as it provides good approximation for short period of time. We plotted the variation of temperature, displacement and stress fields with radial distance for very short period of time for MGL model. Also, we make a comparative graphical analysis with the results predicted by MGL, GL and LS models. We observe that at smaller time and during the initial time of interaction, the physical variables show significantly different behavior under three generalized thermoelasticity theories. We also find the significant impact of velocity of moving heat source and relaxation parameters on behavior of physical variables.

3.3.2 Basic governing equations

The unified basic governing equations for generalised thermoelasticity theories (LS (Lord and Shulman (1967)), GL (Green and Lindsay (1972)) and MGL (Yu et al. (2018)) models) for homogenous, isotropic elastic body in the absence of body force but in the presence of moving heat source (Q) can be expressed in the following forms:
Stress-displacement relation in the absence of external body force:

$$\sigma_{ij,j} = \rho \frac{\partial^2 u_i}{\partial t^2} \tag{3.3.1}$$

Stress-strain temperature relation:

$$\sigma_{ij} = (1 + z_1 \tau_1 \frac{\partial}{\partial t})(2\mu e_{ij} + \lambda e_{kk} \delta_{ij}) - \gamma(\theta + z_2 \tau_1 \frac{\partial \theta}{\partial t})\delta_{ij} \tag{3.3.2}$$

Heat conduction equation in the presence of external heat source:

$$k\theta_{,ii} = \rho c_E\left(\frac{\partial\theta}{\partial t} + z_3\tau_0\frac{\partial^2\theta}{\partial t^2}\right) + \gamma\theta_0\left(\frac{\partial e_{ij}}{\partial t} + z_4\tau_0\frac{\partial^2 e_{ij}}{\partial t^2}\right)\delta_{ij} - \left(1 + z_5\tau_0\frac{\partial}{\partial t}\right)Q \tag{3.3.3}$$

Strain-displacement relation:

$$e_{ij} = \frac{u_{i,j} + u_{j,i}}{2} \tag{3.3.4}$$

On combining Eqs. (3.3.1) and (3.3.2), we obtain

$$\rho\frac{\partial^2 u_i}{\partial t^2} = \left(1 + z_1\tau_1\frac{\partial}{\partial t}\right)\left(2\mu e_{ij} + \lambda e_{kk}\delta_{ij}\right)_{,j} - \gamma\left(\theta + z_2\tau_1\frac{\partial\theta}{\partial t}\right)_{,j}\delta_{ij} \tag{3.3.5}$$

Based on different sets of values of z_1, z_2, z_3, z_4 and z_5, one can obtain the governing equations in the context of different theories as given below:

Case I: LS model: $z_1 = z_2 = 0$ and $z_3 = z_4 = z_5 = 1$.

Case II: GL model: $z_1 = z_4 = z_5 = 0$ and $z_2 = z_3 = 1$.

Case III: MGL model: $z_5 = 0$ and $z_1 = z_2 = z_3 = z_4 = 1$.

3.3.3 Formulation of the problem

In cylindrical coordinate system (r, ϕ, z), we consider the problem of an infinite thermoelastic medium having a cylindrical cavity of radius (R) occupying the region $R \leq r < \infty$. The medium is supposed to be homogeneous and isotropic and subjected to thermal shock at the surface of the cavity. Let us assume that the body has an axisymmetric structure under the axisymmetric load, so the problem is one dimensional and the physical field variable displacement vector has only the radial component $u\,(r, t)$. Temperature field is also dependent on r and t. The components of strain tensor are

therefore given by

$$\varepsilon = \begin{pmatrix} e_{rr} & 0 & 0 \\ 0 & e_{\phi\phi} & 0 \\ 0 & 0 & 0 \end{pmatrix}, e_{rr} = \frac{\partial u}{\partial r}, e_{\phi\phi} = \frac{u}{r}.$$

Further, the stress tensor has only three components σ_{rr}, $\sigma_{\phi\phi}$ and σ_{zz} that are in radial, transverse and axial directions, respectively.

Therefore, one can write the above unified governing equations in the following forms :

The equation of motion :

$$\rho\frac{\partial^2 u}{\partial t^2} = (\lambda + 2\mu)\left(1 + z_1\tau_1\frac{\partial}{\partial t}\right)\left(\frac{\partial e_{kk}}{\partial r}\right) - \gamma\left(1 + z_2\tau_1\frac{\partial}{\partial t}\right)\left(\frac{\partial \theta}{\partial r}\right) \tag{3.3.6}$$

The heat equation :

$$k\triangle\theta = \rho C_E\left(1 + z_3\tau_0\frac{\partial}{\partial t}\right)\left(\frac{\partial \theta}{\partial t}\right) + \gamma T_0\left(1 + z_4\tau_0\frac{\partial}{\partial t}\right)\left(\frac{\partial e_{kk}}{\partial t}\right) - \left(1 + z_5\tau_0\frac{\partial}{\partial t}\right)Q \tag{3.3.7}$$

where $\triangle = \frac{\partial^2}{\partial r^2} + \frac{1}{r}\frac{\partial}{\partial r}$.

Now, the constitutive relations for non-zero stress components can be written as:

$$\sigma_{rr} = \left(1 + z_1\tau_1\frac{\partial}{\partial t}\right)\left[(\lambda + 2\mu)\frac{\partial u}{\partial r} + \lambda\frac{u}{r}\right] - \gamma\left(1 + z_2\tau_1\frac{\partial}{\partial t}\right)\theta \tag{3.3.8}$$

$$\sigma_{\phi\phi} = \left(1 + z_1\tau_1\frac{\partial}{\partial t}\right)\left[(\lambda + 2\mu)\frac{u}{r} + \lambda\frac{\partial u}{\partial r}\right] - \gamma\left(1 + z_2\tau_1\frac{\partial}{\partial t}\right)\theta \tag{3.3.9}$$

$$\sigma_{zz} = \lambda\left(1 + z_1\tau_1\frac{\partial}{\partial t}\right)e - \gamma\left(1 + z_2\tau_1\frac{\partial}{\partial t}\right)\theta \tag{3.3.10}$$

$$\sigma_{zr} = \sigma_{\phi z} = \sigma_{r\phi} = 0$$

The cubical dilatation can be written as:

$$e_{kk} = e = trace\,(\varepsilon) = \frac{\partial u}{\partial r} + \frac{u}{r} \tag{3.3.11}$$

Let us consider that the heat source is moving (Youssef (2009)) with constant velocity v having strength Q_0 and can be expressed as :

$$Q = Q_0 H\,(r - R) \begin{cases} \frac{v}{\sqrt{v^2t^2 - r^2}} & \text{when } R \le r < vt, \\ 0 & \text{when } vt \le r < \infty \end{cases} \tag{3.3.12}$$

For convenience, the following non dimensional variables are used

$$(r', u') = c_0\eta\,(r, u)\,, (t', \tau_0', \tau_1') = c_0^2\eta\,(t, \tau_0, \tau_1)\,, \theta' = \frac{\theta}{T_0},$$

$$\left(\sigma_{rr}', \sigma_{\phi\phi}', \sigma_{zz}'\right) = \frac{1}{\mu}\left(\sigma_{rr}, \sigma_{\phi\phi}, \sigma_{zz}\right), Q_0' = \frac{Q_0}{T_0\rho C_E}, v' = \frac{v}{c_0}$$

where $n = \frac{\rho c_E}{k}$ and $c_0 = \sqrt{\left(\frac{\lambda+2\mu}{\rho}\right)}$.

After dropping superscripted primes for convenience, the Eqs. (3.3.6-3.3.10) are reduced to

$$\frac{\partial^2 u}{\partial t^2} = \left(1 + z_1\tau_1\frac{\partial}{\partial t}\right)\left(\frac{\partial e}{\partial r}\right) - b\left(1 + z_2\tau_1\frac{\partial}{\partial t}\right)\left(\frac{\partial \theta}{\partial r}\right) \tag{3.3.13}$$

$$\triangle\theta = \left(1 + z_3\tau_0\frac{\partial}{\partial t}\right)\left(\frac{\partial \theta}{\partial t}\right) + \varepsilon\left(1 + z_4\tau_0\frac{\partial}{\partial t}\right)\left(\frac{\partial e}{\partial t}\right) - \left(1 + z_5\tau_0\frac{\partial}{\partial t}\right)Q \tag{3.3.14}$$

$$\sigma_{rr} = \left(1 + z_1\tau_1\frac{\partial}{\partial t}\right)\left[\beta^2\frac{\partial u}{\partial r} + \left(\beta^2 - 2\right)\frac{u}{r}\right] - \alpha_0\left(1 + z_2\tau_1\frac{\partial}{\partial t}\right)\theta \tag{3.3.15}$$

$$\sigma_{\phi\phi} = \left(1 + z_1\tau_1\frac{\partial}{\partial t}\right)\left[\beta^2\frac{u}{r} + \left(\beta^2 - 2\right)\frac{\partial u}{\partial r}\right] - \alpha_0\left(1 + z_2\tau_1\frac{\partial}{\partial t}\right)\theta \tag{3.3.16}$$

$$\sigma_{zz} = \left(\beta^2 - 2\right)\left(1 + z_1\tau_1\frac{\partial}{\partial t}\right)e - \alpha_0\left(1 + z_2\tau_1\frac{\partial}{\partial t}\right)\theta \tag{3.3.17}$$

where $\alpha_0 = \frac{\gamma T_0}{\mu}, \beta = \sqrt{\left(\frac{\lambda+2\mu}{\mu}\right)}, b = \frac{\alpha_0}{\beta^2}$

Now, we apply $\frac{\partial}{\partial r} + \frac{1}{r}$ to Eq. (3.3.13), we get

$$\frac{\partial^2 e}{\partial t^2} = \left(1 + z_1\tau_1\frac{\partial}{\partial t}\right)(\triangle e) - b\left(1 + z_2\tau_1\frac{\partial}{\partial t}\right)(\triangle\theta) \tag{3.3.18}$$

Applying Laplace transform to Eqs. (3.3.14-3.3.18) and taking into the account that the medium described here is quiescent initially, we obtain

$$s^2\overline{e} = z_{11}\left(\triangle\overline{e}\right) - bz_{21}\left(\triangle\overline{\theta}\right) \tag{3.3.19}$$

$$\triangle\overline{\theta} = z_{30}s\overline{\theta} + \varepsilon z_{40}s\overline{e} - z_{50}wK_0\left(\frac{sr}{v}\right) \tag{3.3.20}$$

$$\overline{\sigma}_{rr} = z_{11}\left[\beta^2\frac{\partial u}{\partial r} + \left(\beta^2 - 2\right)\frac{u}{r}\right] - \alpha_0 z_{21}\overline{\theta} \tag{3.3.21}$$

$$\overline{\sigma}_{\phi\phi} = z_{11}\left[\beta^2\frac{u}{r} + \left(\beta^2 - 2\right)\frac{\partial u}{\partial r}\right] - \alpha_0 z_{21}\overline{\theta} \tag{3.3.22}$$

$$\overline{\sigma}_{zz} = \left(\beta^2 - 2\right)z_{11}\left(\frac{\partial u}{\partial r} + \frac{u}{r}\right) - \alpha_0 z_{21}\overline{\theta} \tag{3.3.23}$$

where $z_{11} = (1 + z_1\tau_1 s), z_{21} = (1 + z_2\tau_1 s), z_{30} = (1 + z_3\tau_0 s), z_{40} = (1 + z_4\tau_0 s), z_{50} = (1 + z_5\tau_0 s), w = Q_0 H(r - R)$ and s denotes the Laplace transform parameter.

Substituting from Eq. (3.3.20) to Eq. (3.3.19), yields

$$(\triangle - \alpha_2)\, e = \frac{z_{21}z_{30}bs}{z_{11}}\overline{\theta} - \frac{z_{21}z_{50}bw}{z_{11}}K_0\left(\frac{sr}{v}\right) \tag{3.3.24}$$

where $\alpha_2 = \frac{s^2 + b\varepsilon z_{21}z_{40}}{z_{11}}$

Eq. (3.3.20) can be re-written as

$$(\triangle - z_{30}s)\,\overline{\theta} = \varepsilon z_{40} s\overline{e} - z_{50} w K_0\left(\frac{sr}{v}\right) \tag{3.3.25}$$

Eliminating $\overline{e}$ from Eq. (3.3.24) and (3.3.25), we get

$$\left(\triangle^2 - L\triangle + M\right)\overline{\theta} = \alpha_3 K_0\left(\frac{sr}{v}\right) \tag{3.3.26}$$

where $L = \alpha_2 + sz_{30}, M = \alpha_2 s z_{30} - \varepsilon b s^2 \frac{z_{21} z_{31} z_{40}}{z_{11}}, \alpha_3 = w\left(\alpha_2 z_{50} - z_{50}\left(\frac{s}{v}\right)^2 - \varepsilon b s \frac{z_{21} z_{50} z_{40}}{z_{11}}\right)$

In a similar manner, we get that $\overline{e}$ satisfies the following differential equation:

$$\left(\triangle^2 - L\triangle + M\right)\overline{\theta} = \alpha_4 K_0\left(\frac{sr}{v}\right) \tag{3.3.27}$$

where $\alpha_4 = -bw\left(\frac{s}{v}\right)^2 \frac{z_{21} z_{50}}{z_{11}}$

Let $P_i\,(i = 1, 2, 3, 4)$ be the roots of the following characteristic equation:

$$x^4 - Lx^2 + M = 0 \tag{3.3.28}$$

with $P_1 = -P_3, P_2 = -P_4$.

Then the solution of Eqs. (3.3.24) and (3.3.26), which is bounded at infinity $(r \to \infty)$ can be written as

$$\overline{\theta} = c_1 K_0\left(\frac{sr}{v}\right) + \sum_{i=1}^{2} A_i\left(P_i^2 - \alpha_2\right) K_0\left(P_i r\right) \tag{3.3.29}$$

$$\overline{e} = c_2 K_0\left(\frac{sr}{v}\right) + \sum_{i=1}^{2} B_i K_0\left(P_i r\right) \tag{3.3.30}$$

where $c_1 = \frac{\alpha_3}{\left(\frac{s}{v}\right)^4 - L\left(\frac{s}{v}\right)^2 + M}$, and A_i, B_i are arbitrary constants depending on the parameter s.

Now we substitute the expressions from Eqs. (3.3.29), (3.3.30) into Eq. (3.3.24) to obtain the following relations:

$$B_i = bs\frac{z_{21}z_{30}}{z_{11}}A_i \;\; i = 1, 2 \tag{3.3.31}$$

$$c_2 = \frac{bz_{21}}{z_{11}}\left(\frac{sz_{30}c_1 - wz_{50}}{\left(\frac{s}{v}\right)^2 - \alpha_2}\right). \tag{3.3.32}$$

Substituting Eq. (3.3.31) into Eq. (3.3.30), we get

$$\overline{e} = c_2 K_0\left(\frac{sr}{v}\right) + \sum_{i=1}^{2} bs\frac{z_{21}z_{30}}{z_{11}}A_i K_0\left(P_i r\right) \tag{3.3.33}$$

Now we derive the expression for $\overline{u}$ by using Eq. (3.3.11), as

$$\overline{u} = \frac{1}{r}\int r\overline{e}dr$$

which yields

$$\overline{u} = -\frac{vc_2}{s}K_1\left(\frac{sr}{v}\right) - bs\frac{z_{21}z_{30}}{z_{11}}\sum_{i=1}^{2}\frac{A_i K_1\left(P_i r\right)}{P_i} \tag{3.3.34}$$

Substituting Eqs. (3.3.29), (3.3.33) and (3.3.34) into Eqs. (3.3.21), (3.3.22) and (3.3.23), we further get the expressions of the field variable in the Laplace transform domain as

$$\begin{aligned}\overline{\sigma}_{rr} = {} & \left(z_{11}\beta^2 c_2 - \alpha_0 z_{21}c_1\right)K_0\left(\frac{sr}{v}\right) + \frac{2vc_2}{rs}z_{11}K_1\left(\frac{sr}{v}\right) + \\ & \sum_{i=1}^{2}\left[\left\{bs\beta^2 z_{21}z_{30} - \alpha_0 z_{21}\left(P_i^2 - \alpha_2\right)\right\}K_0\left(P_i r\right) + 2bs\frac{z_{21}z_{30}}{P_i r}K_1\left(P_i r\right)\right]A_i\end{aligned} \tag{3.3.35}$$

$$\begin{aligned}\overline{\sigma}_{\phi\phi} = {} & \left\{z_{11}\left(\beta^2 - 2\right)c_2 - \alpha_0 z_{21}c_1\right\}K_0\left(\frac{sr}{v}\right) - \frac{2vc_2}{rs}z_{11}K_1\left(\frac{sr}{v}\right) + \\ & \sum_{i=1}^{2}\left[\left\{bs\left(\beta^2 - 2\right)z_{21}z_{30} - \alpha_0 z_{21}\left(P_i^2 - \alpha_2\right)\right\}K_0\left(P_i r\right) - 2bs\frac{z_{21}z_{30}}{P_i r}K_1\left(P_i r\right)\right]A_i\end{aligned} \tag{3.3.36}$$

$$\overline{\sigma}_{zz} = \left\{ z_{11}\left(\beta^2 - 2\right) c_2 - \alpha_0 z_{21} c_1 \right\} K_0\left(\frac{sr}{v}\right) + \sum_{i=1}^{2} \left\{ bs\left(\beta^2 - 2\right) z_{21} z_{30} - \alpha_0 z_{21}\left(P_i^2 - \alpha_2\right) \right\} K_0\left(P_i r\right) A_i \tag{3.3.37}$$

Boundary conditions: Now we consider that the boundary of the cavity ($r = R$) is traction free along radial direction and subjected to thermal shock, which is expressed as:

$$\theta\left(R,t\right) = \theta_0 H\left(t\right), \sigma_{rr}\left(R,t\right) = 0 \tag{3.3.38}$$

where θ_0 is a constant and $H\left(t\right)$ is Heaviside unit step function.

In Laplace transform domain, Eq. (3.3.33) can be written as

$$\overline{\theta}\left(R,s\right) = \frac{\theta_0}{s}, \overline{\sigma}_{rr}\left(R,s\right) = 0 \tag{3.3.39}$$

Using the boundary conditions in Eqs. (3.3.29) and (3.3.35) to determine the unknown parameters, we have

$$A_1 = \frac{S_2 U - L_2 T}{S_1 L_2 - S_2 L_1} \tag{3.3.40}$$

$$A_2 = \frac{T L_1 - U S_1}{S_1 L_2 - S_2 L_1} \tag{3.3.41}$$

where

$$S_i = \left(P_i^2 - \alpha_2\right) K_0\left(P_i R\right) \quad i = 1, 2, \tag{3.3.42}$$

$$L_i = \left[\left\{ bs\beta^2 z_{21} z_{30} - \alpha_0 z_{21}\left(P_i^2 - \alpha_2\right) \right\} K_0\left(P_i R\right) + 2bs \frac{z_{21} z_{30}}{P_i r} K_1\left(P_i R\right) \right] \quad i = 1, 2, \tag{3.3.43}$$

$$T = c_1 K_0\left(\frac{sR}{v}\right) - \frac{\theta_0}{s}, \tag{3.3.44}$$

$$U = \left(z_{11}\beta^2 c_2 - \alpha_0 z_{21} c_1\right) K_0\left(\frac{sR}{v}\right) + \frac{2vc_2}{Rs} z_{11} K_1\left(\frac{sR}{v}\right). \tag{3.3.45}$$

In Eqs. (3.3.29, 3.3.34, 3.3.35, 3.3.36 and 3.3.37) different sets of values of $z_{11}, z_{21}, z_{30}, z_{40}$

and z_{50} implicitly represent the solutions of the problem for three different generalized thermoelastic models namely, LS, GL and MGL models in the Laplace transform domain.

The solutions in the context of a particular model can be extracted for different values of parameters z_1, z_2, z_3, z_4 and z_5 as mentioned above.

3.3.4 Numerical implementation and result discussion

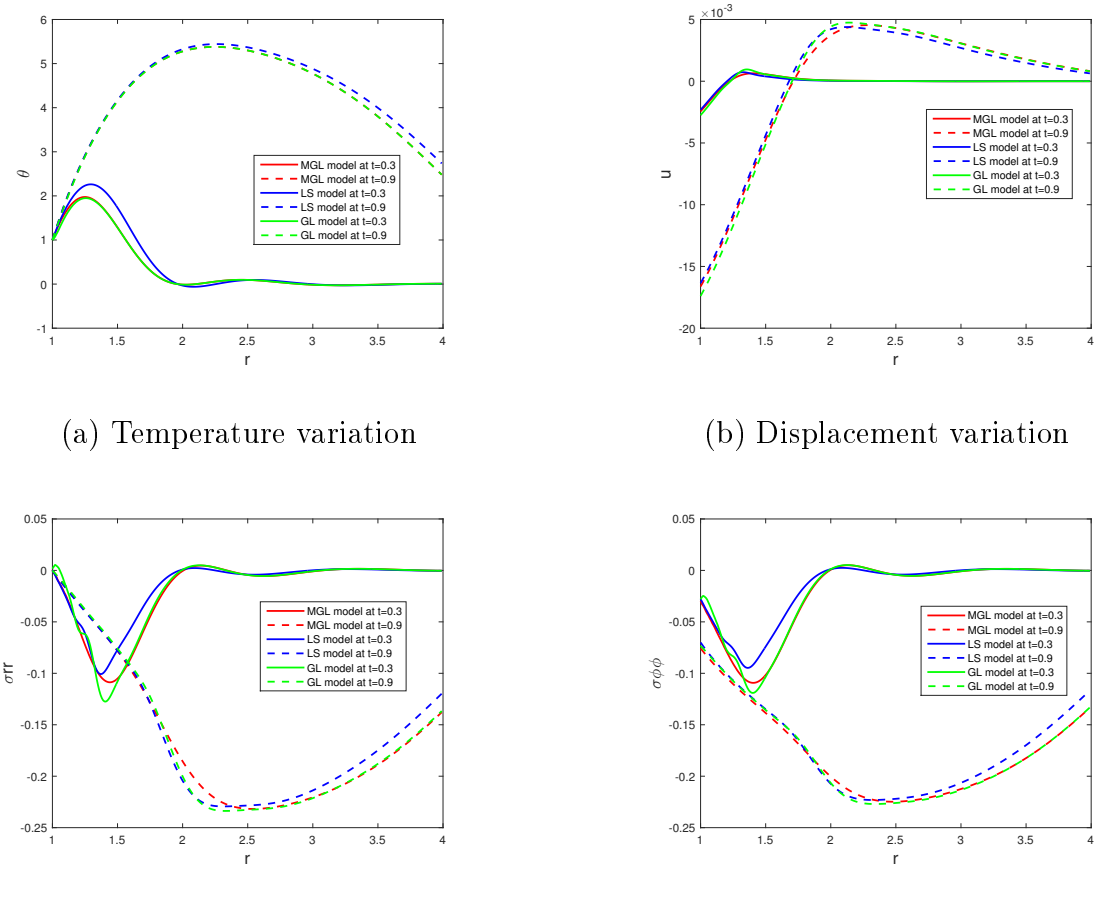

(a) Temperature variation

(b) Displacement variation

(c) Radial stress variation

(d) Circumferential stress variation

Figure 3.3.1: Comparison of LS, GL and MGL model at time $t = 0.3$ and 0.9.

The main objective of this subsection is that we numerically estimate the influence of the strain rate as well as the temperature rate terms on the present problem and finally understand the effect of moving heat source with transient heating condition

under MGL model. For this, the solution in the Laplace transform system obtained in the previous section yields the time-dependent solution of the original thermoelastic system via application of the inverse Laplace transform, which is conducted numerically by using the Stehfest algorithm with MATLAB programming. This method provides fast and very accurate approximation for transient responses. We plot the variations of all field variables for the present problem in physical domain (r, t) and compare the results obtained under different generalized thermoelastic models (LS and GL and MGL models).

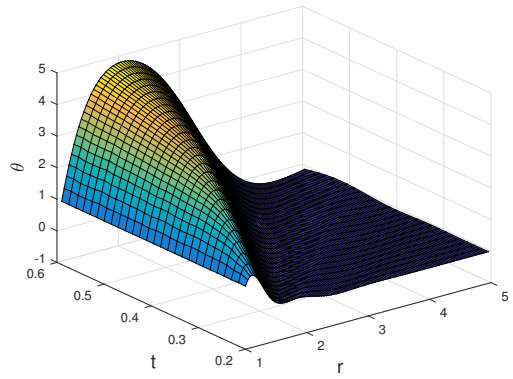

(a) Temperature variation

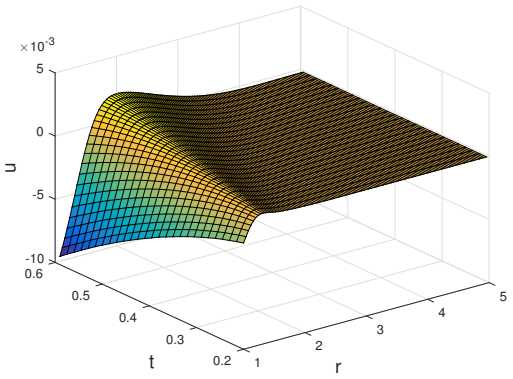

(b) Displacement variation

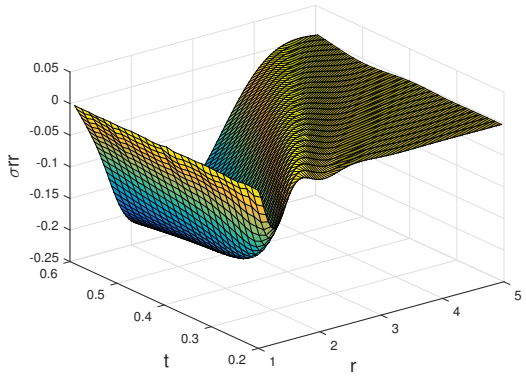

(c) Radial stress variation

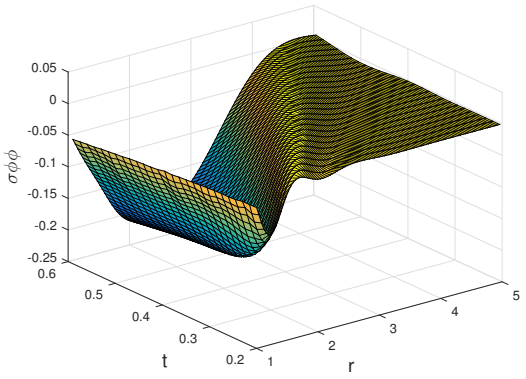

(d) Circumferential stress variation

Figure 3.3.2: Three dimensional variations of field variables at $t = 0.3$ to 0.6.

The non-dimensional physical quantities such as temperature, displacement and

stress components depend not only on two relaxation time parameters of the material but also on the velocity of heat source. The numerical results are obtained and their graphical representations are carried out for three cases as displayed in Figs. (3.3.1-3.3.5). The following important facts are observed:

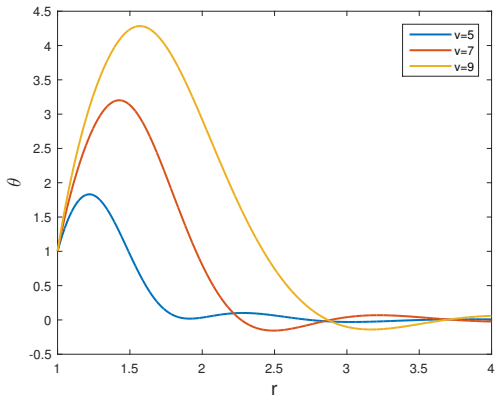

(a) Temperature variation

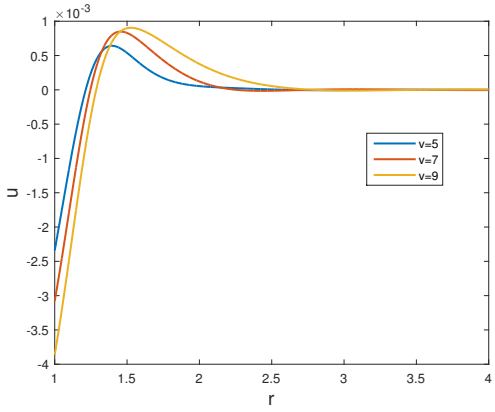

(b) Displacement variation

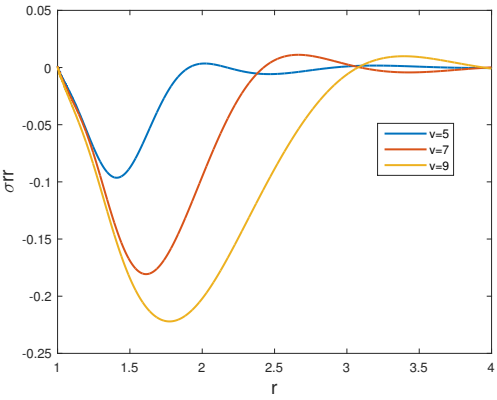

(c) Radial stress variation

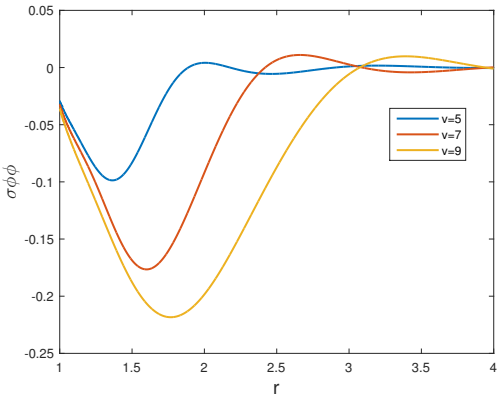

(d) Circumferential stress variation

Figure 3.3.3: Variation of field variables at different velocity of heat source for MGL model at $t = 0.3$.

I. Figures 3.3.1 (a,b,c,d) reveal the nature of variations in field quantities in the contexts of the three different theories and at two different instants of time i.e. at $t = 0.3$ and 0.9. For showing these results, we fix the velocity of heat source as $v = 5$. One can observe that all three models predict significantly different values of field quantities for

small time and this difference is significant near the boundary of the cavity and more prominent near the extremum values. Difference is more prominent for the cases of two stress components. As time increases, the difference obtained between the results for three models is observed to be negligible.

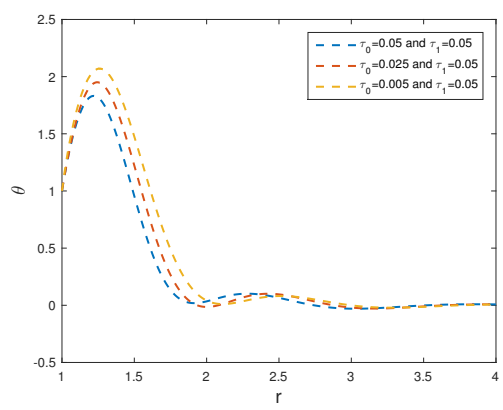

(a) Temperature variation

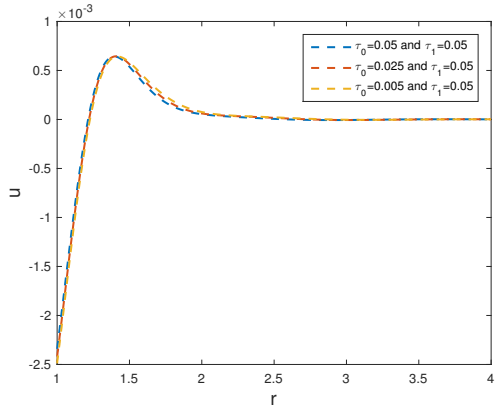

(b) Displacement variation

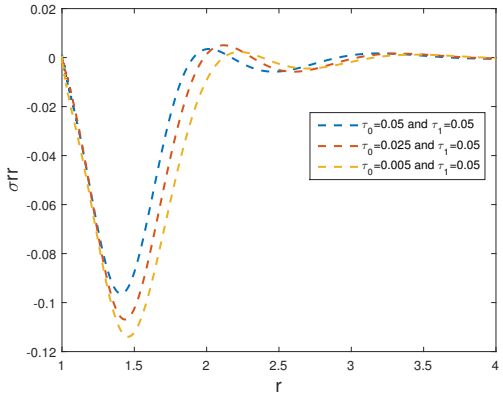

(c) Radial stress variation

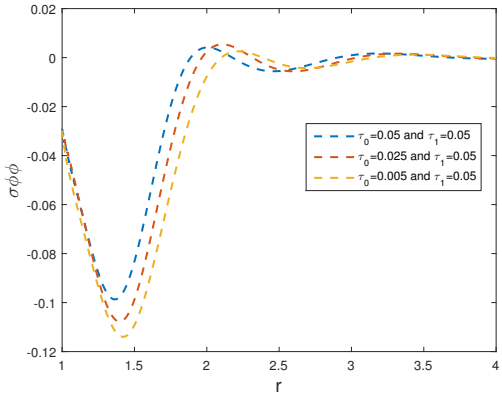

(d) Circumferential stress variation

Figure 3.3.4: Variations of field variables at different τ_0 for MGL model.

This implies that during the initial time of interaction due to heat source and thermal shock at the boundary, the application of thermoelastic model plays a very significant role and indicate different natures of thermal and elastic waves propagating through the material. LS model and GL model predict the lowest values and highest values, respectively for each of the field variables. The values under MGL model are in between

the values given by other two models.

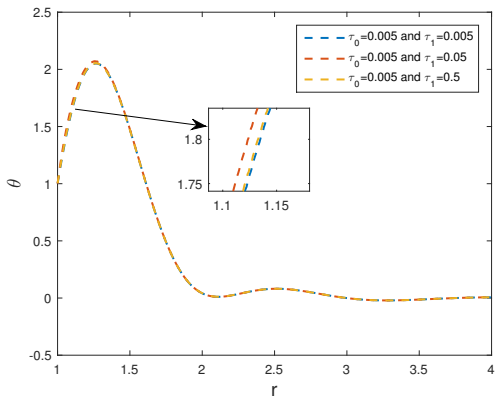

(a) Temperature variation

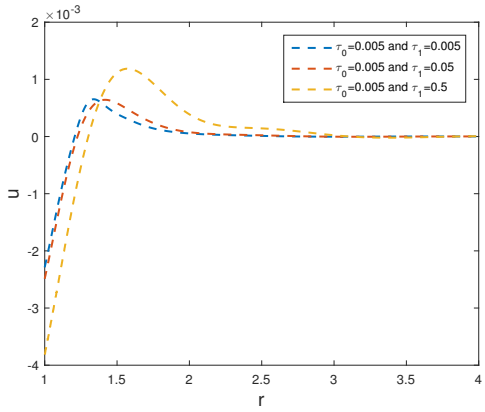

(b) Displacement variation

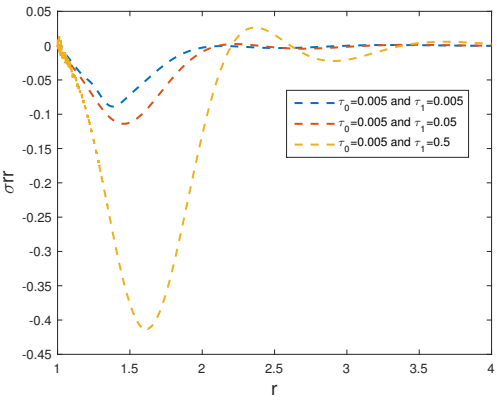

(c) Radial stress variation

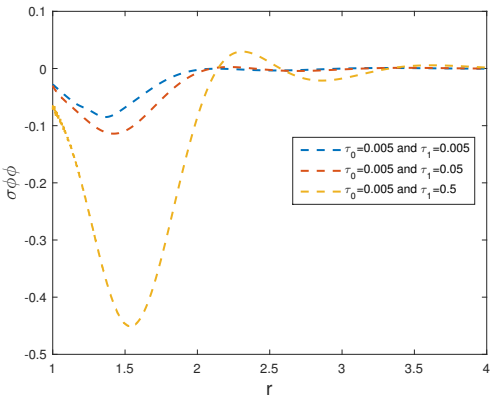

(d) Circumferential stress variation

Figure 3.3.5: Variations of field variables at different τ_1 for MGL model.

II. The 3-Dimensional figures 3.3.2 (a,b,c,d) show the variation of temperature, displacement and stress components with radial distance during the short period of time interval ($t = 0.3$ to $t = 0.6$) for MGL model. Figure 3.3.2 (a), shows that the temperature distribution satisfies the boundary condition. It increases in the beginning to achieve its maximum amplitude, then decreases to vanish finally. Figure 3.3.2 (b) depicts that the displacement starts with negative values and its value increases at the beginning to achieve its maximum amplitude, then again decreases to zero. Figures 3.3.2 (c,d) indicates that the radial stress satisfies the boundary condition. Both the

stresses are found to be mostly compressive in nature and their absolute values gradually increase to achieve their peak values and then start decreasing to finally become zero. One can further note that at larger time, the peak values of temperature, displacement and absolute value of thermal stresses increase and shift towards right.

III. Figures 3.3.3 (a,b,c,d) display the results for the physical fields in the context of MGL model. Here we investigated the effect of velocity of moving heat source on the distributions of different field variables like displacement, temperature, and radial and circumferential stress components with respect to radial distance at a fixed time ($t = 0.3$). It is observed that the velocity, v has a significant effect on each field variable. Figure 3.3.3 (a) clearly shows that the temperature increases with an increase in velocity at every specified location for the same instant of time. Similar effects are observed for other fields. Figures 3.3.3 (a,b,c,d) indicate that for higher values of speed, the peak values of temperature, displacement and the stress components shift towards right. The peak values of field variables are found because the heat source energy blow up close to point $r = vt$ and after that point its effect is vanished as shown by Eq. 3.3.12. It can be seen from all four figures 3.3.3 (a,b,c,d) that the domain of influence of each of the physical fields increases as the source speed increases.

IV. In figures (3.3.4, 3.3.5), we determine the effects of relaxation time parameters (τ_0 and τ_1) on field variables for the case of MGL model. It is found that when we fix the value of the relaxation parameter τ_1, then τ_0 plays the most significant role for temperature and stress components. As we decrease the τ_0, the temperature, as well as stress components increase and correspondingly the domain of influence for affected region increases significantly. The displacement field is observed to be less affected due to the variation of τ_0. However, the variation in τ_1, by keeping the value of τ_0 fixed, has negligible effect on temperature field, where as τ_1 plays quite significant role for the displacement and stress components. Here, the displacement starts with higher numerical value for larger τ_1. The stress fields are largely affected due to the variations

of both the relaxation parameters. It is clearly observed that both the compressive stresses show higher numerical values for smaller τ_0 and for larger τ_1 as shown in figures (3.3.4, 3.3.5)

3.3.5 Conclusion

In the present subchapter we study a problem of moving heat source under the applications of three generalized thermoelastic models (LS, GL and MGL models). The solutions are obtained by formulating the problem with unified governing equations and constitutive relations for these theories. Numerical results are obtained to have a detailed analysis of the effects of above-mentioned terms in order to understand the results under a recent thermoelasticity theory as compared to the corresponding results under other existing theories. Major highlights of the present investigation may be summarized as follows:

- If the heat source moves with larger speed, the peak values of temperature, displacement and the absolute values of stresses increase and they are attained at larger distance from the boundary. This implies an increase in the domain of influence with the increase of the velocity of heat source.

- In the presence of strain and temperature rate terms under MGL thermoelasticity theory, the relaxation time parameters are found to play significant role. The parameter τ_0 shows a prominent effect on temperature with a small effect on displacement. However, the effect of τ_1 is opposite. It has less effect on temperature but prominent effect on displacement field. The stress components are affected significantly by the variation of both the relaxation parameters. Furthermore, the parameters τ_0 and τ_1 play opposite role on the distributions of both the stress components. The absolute values of radial as well as circumferential stress components increase with the increase of τ_1, where as they are decreased with a increase in τ_0.

- At larger time of interaction, the difference in results of the physical field variables predicted by three models becomes negligible. However, the behavior of field variables during initial time of interaction are largely dependent on the thermoelastic model applied for studying the problem. The disagreement of models in distributions of the field variables is more prominent near the boundary of the cavity that is subjected to a thermal shock. MGL model show much smaller numerical values of variables but greater than LS model, the GL model showing the largest numerical values of each field.

The work is believed to be helpful for practical engineering problems to understand how one can choose a thermoelastic model as the solutions are observed to be largely dependent on the parameters involved in a particular model. The speed of heat source inside the medium is observed to play an important role in the elastic and thermal changes of the medium.